

# Long-range atmospheric transport of persistent organochlorinated compounds from south and mainland south-eastern Asia to a remote mountain site in south-western China

Yue Xu,<sup>ac</sup> Gan Zhang,<sup>\*a</sup> Jun Li,<sup>a</sup> Paromita Chakraborty,<sup>a</sup> Hua Li<sup>b</sup> and Xiang Liu<sup>a</sup>

Received 15th June 2011, Accepted 8th August 2011

DOI: 10.1039/c1em10470e

A range of organochlorinated compounds have been consumed in China, India and the countries of mainland southeast Asia (MSA). Considering their persistence in the environment and ability in long-range atmospheric transport (LRAT), the potential outflow of these compounds from this region is therefore of great concern in the context of the global distribution of toxic chemicals. As part of a monitoring campaign aimed at investigating the LRAT of organochlorine pesticides (OCPs) and polychlorinated biphenyls (PCBs) from southern China, MSA and northern India, atmospheric levels of OCPs and PCBs were measured once a week from October 2005 through December 2006 at Tengchong Mountain (TM), a remote site located in south-western China. The average concentrations of OCPs were found to be higher than those in other remote stations in the Arctic and the Tibetan plateau, except for  $\alpha$ -hexachlorocyclohexane ( $\alpha$ -HCH). A high level of  $\beta$ -HCH and low  $\alpha$ -HCH/ $\beta$ -HCH ratio was attributed to an accidental release of  $\beta$ -HCH from unknown sources, besides obvious evidence of lindane ( $\gamma$ -HCH) and technical HCH usage. Temporal variations of chlordanes and endosulfan were related to the usage pattern of these compounds, as well as LRAT. In contrast, dichlorodiphenyltrichloroethane (DDT) exhibited a relatively minor seasonal variation. The OCP levels at the monitoring site were found to be related to the air parcel back trajectories on the basis of four distinct clusters. Elevated levels of HCHs and DDTs were observed when air parcels originated from northern India where considerable OCP usage was reported recently, while high levels of  $\gamma$ -HCH and TC (*trans*-chlordanes) were mainly associated with air masses from southern China and northern MSA. The study highlighted the high background level of OCPs as well as their temporal patterns of *trans*-boundary LRAT in the MSA region.

## 1. Introduction

Countries in tropical Asia consume a large amount of organochlorinated compounds. Agriculture is a major livelihood there and agricultural output in countries of this region accounted for over 35% of the world cereal production and over 48% of fruits and vegetables (FAO, 2004). Hence, pesticides have been extensively used to increase crop yield. The monsoon climate

<sup>a</sup>State Key Laboratory of Organic Geochemistry, Guangzhou Institute of Geochemistry, Chinese Academy of Sciences, Guangzhou, 510640, China. E-mail: zhanggan@gig.ac.cn; Fax: +86-20-8529-0130; Tel: +86-20-8529-0805

<sup>b</sup>School of Resource and Environmental Engineering, WuHan University of Technology, WuHan, China 430074

<sup>c</sup>Graduate University of Chinese Academy of Sciences, Beijing, 100080, China

### Environmental impact

Organochlorinated compounds in tropical Asia are of scientific concern due to their large historical and ongoing usage. The emitted airborne pollutants could be subject to impacts of the prevailing Asian monsoon in this region and undergo long-range atmospheric transport, yet limited studies had been conducted to elucidate transport characteristics and identify potential sources. This article presents a year-long study of organochlorinated compounds at a remote station in the south-western part of China. Besides routine monitoring, potential source contribution function and trajectory cluster analysis were performed to determine the origin of the chemicals. The results in this study could extend our knowledge on the *trans*-boundary transport patterns of organochlorinated compounds in the atmosphere over tropical Asia, including India, northern MSA and southern China.

could also influence the usage pattern of pesticides in tropical Asia. With relatively low rainfall, spring (from February to April) and winter (from September to January of next year) are planting seasons, possibly leading to greater use of pesticides. Previous reports demonstrate that concentrations of OCPs (organochlorine pesticides) rise in spring and winter and decline in the rainy season (from May to August), which coincides with the time of local agriculture activities.<sup>1</sup> Furthermore, floods and tropical storms frequently devastating the region could create breeding grounds for mosquitoes and thus frequently lead to pesticide usage for vector control after such disasters.<sup>2,3</sup> Historical usage of pesticides in many countries of this region was estimated to account for a large part of total global usage.<sup>4</sup> Although some pesticides were banned or highly restricted, residues of pesticides of the past and current application make it a distinct OCP source region of global significance. In addition, recent emission from PCB-containing equipment, large-scale land transformation,<sup>5</sup> growing ship breaking and e-waste recycling<sup>6</sup> in countries of the region confront them with escalating PCB (polychlorinated biphenyls) issues, some of which could even lead to a sharp rise of PCB fluxes in recent sediments.<sup>5</sup>

Owing to uncertainties in sources and pathways under a tropical monsoon climate, the distribution, behavior and fate of those contaminants are not well understood. Previous studies show that local pollution in southern China and India could be significant,<sup>5,6</sup> however data from other areas is difficult to obtain,<sup>7</sup> and only limited studies are available from countries in MSA.<sup>8,9</sup> For instance, data on pesticide pollution in Myanmar are still scarce, even though its agriculture sector contributed 57.2% of its GDP (FAO, 2004). There is evidence that the emitted pollutants could transport to remote sites *via* air mass movement.<sup>10</sup> Therefore, research on environmental fate and exposure of OCPs and PCBs in tropical Asia is also an important part of the global study on persistent organic pollutants (POPs).

Air monitoring at remote sites is one of the major ways to assess the relative importance of sources on a regional scale and study the environmental fate of pollutants, because local source can be ignored there and LRAT (long-range atmospheric transport) could be the most important pathway of pollutant input.<sup>11</sup> Numerous campaigns have been conducted in remote areas, such as the Arctic,<sup>12,13</sup> the Antarctic<sup>14</sup> and Mt. Everest region,<sup>15</sup> to trace the concentrations, temporal and spatial variations, and distant pollution sources of organochlorinated compounds. To increase our knowledge of the environmental fate and transport of toxic chemicals in tropical Asia, a field campaign was conducted at a tropical mountain monitoring site. Tengchong Mountain (TM) is an observatory of the Global Climate Observing System (GCOS), WMO, where a variety of measurements are being conducted to study the atmospheric transport of various pollutants in MSA and China.<sup>16</sup> This site is located under the regimes of both East Asian and Indian monsoon and thus influenced mainly by air masses from China, India and MSA. Given its minor seasonal variation in air temperature, it is an ideal receptor site to monitor atmospheric transport of OCPs and PCBs from the three regions.

In this paper, we report the results from a year-round weekly monitoring of OCPs and PCBs at TM. In conjunction with air mass back trajectory and potential source contribution function (PSCF) analysis, the temporal patterns of *trans*-boundary OCP

transport in the atmosphere over MSA were also elucidated and assessed.

## 2. Materials and analytical methods

### 2.1. Sampling site and collection

Air samples were collected on the top of Tengchong Mountain (24.95 N, 98.48 E, 1960 m a.s.l.), located in Yunnan Province in southwest China, close to the eastern part of the Tibetan Plateau (Fig. 1). The sampling site is situated ~10 km to the south of Tengchong town, with a population of 44 000, and is surrounded by hills and a few small villages.<sup>17</sup>

24 h air samples of ~430 m<sup>3</sup> were taken once every 7 days from 22 October 2005 to 27 December 2006. A total of 56 samples were collected as a few samples were lost during storage and transportation. Air was pulled through a quartz microfiber filter (QFF) (QMA, 20.3 × 25.4 cm, Whatman, Maidstone, England) and a pre-cleaned polyurethane foam (PUF) plug (6.5 cm diameter, 7.5 cm length, 0.030 g cm<sup>-3</sup> density) using a modified Anderson-type high volume sampler. The QFFs were baked in a muffle furnace at 450 °C for 4 h. The PUF plugs were pre-cleaned twice by Accelerated Solvent Extraction with a mixture (1 : 1, v/v) of acetone and dichloromethane (DCM) at 100 °C and 1500 psi for 15 min. After sampling, all the samples were wrapped with clean aluminium foil, sealed in Teflon bags, and kept at -18 °C prior to analysis. The details of sampling and analysis are described in a previous study.<sup>18</sup>

### 2.2. Extraction and analysis

All the collected filter and PUF plug samples were Soxhlet extracted with dichloromethane (DCM) separately for 24 h, spiked with 10 ng of 2,4,5,6-tetrachloro-*m*-xylene (TCmX), PCB 30, PCB 198 and PCB 209 as surrogates. Activated copper granules were added to the collection flask to remove elemental sulphur. Each sample extract was concentrated by a rotary evaporator and solvent-exchanged into hexane. The elute was cleaned up through an 8 mm i.d. alumina/silica column in turn containing anhydrous sodium sulphate (1 cm), 50% sulfuric acid

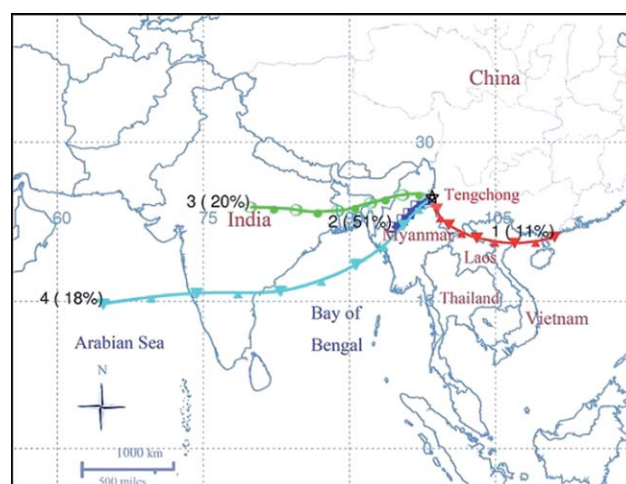


Fig. 1 Map of sampling station and four types of clusters of air mass backward trajectories.

silica (2 cm), neutral silica gel (3 cm, 3% deactivated) and neutral alumina (3 cm, deactivated with 3% water). OCPs were eluted with 15 ml of a mixture of dichloromethane and hexane (1 : 1, v/v). The eluent solvent was removed under a gentle stream of nitrogen and exchanged into 25  $\mu\text{L}$  of dodecane. Prior to sealing, 20 ng of pentachloronitrobenzene (PCNB) and PCB 54 were added into each sample as internal standards.

OCPs were analyzed with an Agilent 6890 gas chromatograph equipped with a capillary column (CP-Sil 8 CB, 50 m, 0.25 mm, 0.25  $\mu\text{m}$ ) and an electron capture detector (ECD). Samples (1  $\mu\text{L}$ ) were injected under splitless mode. High purity nitrogen was used as carrier and detector make-up gas with a flow rate of 1.1 ml  $\text{min}^{-1}$  and 60 ml  $\text{min}^{-1}$ , respectively. The injector temperature was 250  $^{\circ}\text{C}$ . The initial oven temperature was set at 60  $^{\circ}\text{C}$  for 1 min and raised to 180  $^{\circ}\text{C}$  at a rate of 7  $^{\circ}\text{C min}^{-1}$ , from 180  $^{\circ}\text{C}$  to 205  $^{\circ}\text{C}$  at 3  $^{\circ}\text{C min}^{-1}$ , from 205  $^{\circ}\text{C}$  to 290  $^{\circ}\text{C}$  at 6  $^{\circ}\text{C min}^{-1}$ , and held for 30 min.

PCBs were analyzed with an Agilent 7890A gas chromatograph equipped with a capillary column (VARIAN, CP-Sil 8 CB, 50 m, 0.25 mm, 0.25  $\mu\text{m}$ ). The detector was a 5975C inert XL MSD operating in the selected ion mode (SIM). The temperature of MSD source was 230  $^{\circ}\text{C}$  and that of the quadrupole 150  $^{\circ}\text{C}$ . Samples (1  $\mu\text{L}$ ) were injected under splitless mode with a 12 min solvent delay time. High purity helium was used as carrier gas with a flow velocity of 1.83 ml  $\text{min}^{-1}$ . The injector temperature was 250  $^{\circ}\text{C}$ . The initial oven temperature was set at 150  $^{\circ}\text{C}$  for 3 min and raised to 290  $^{\circ}\text{C}$  at a rate of 4  $^{\circ}\text{C min}^{-1}$ , and held for 20 min.

### 2.3. Quality control

The stability of GC-ECD and GC-MS was checked daily using two series of OCPs and PCBs standards and relative standard deviation was less than 10%. Lab blanks were pre-cleaned PUF plugs and filters. Field blanks were obtained by transporting and handling pre-cleaned PUF plugs and filters in exactly the same way as samples, while introducing no air. Lab and field blanks were subject to the same storage and analytical procedures as samples. The amount of all the compounds discussed below in field blanks was less than 5% of the amount in the samples. Almost all target compounds were collected in the first PUF plug in the breakthrough tests at sampling temperature. Potential breakthrough may happen when using PUF to trap HCB and HCH in the gaseous phase, however, a separate test using tandem PUFs showed that the breakthrough was within 10%. Only  $\gamma$ -HCH, *p,p'*-DDT and endosulfan sulfate can be detected in filter samples, thus the concentrations reported for these three compounds are the sum of the concentrations in filters and PUFs, while the concentrations of other compounds discussed are the data measured in PUF samples.

The surrogates described above were analyzed to determine procedural recoveries of OCPs and PCBs. Recoveries for TCmX, PCB 30, PCB 198 and PCB 209 were 76%  $\pm$  9.3%, 69%  $\pm$  7.5%, 73%  $\pm$  13% and 89%  $\pm$  8.7%, respectively. Data were recovery corrected in this study.

### 2.4. Back trajectory

Five-day air parcel back trajectories were calculated five times a day (0, 6, 12, 18 and 24 UTC) of sampling days by the

Hybrid-Single Particle Integrated Trajectories (HYSPLIT 4.8), provided by the National Oceanic and Atmospheric Administration (NOAA) Air Resource Laboratory. Each trajectory was estimated at 100 m above ground level and was cross checked at 500 m and 1000 m above ground level. In order to determine pollutant sources, all the air mass back trajectories were clustered into four types by HYSPLIT 4.8 (Fig. 1). Cluster 1, 2, 3 and 4 represented air masses originating in southeastern China, Myanmar, central India, and the Bay of Bengal respectively.

Cluster 4 had the highest relative humidity while type 3 cluster had the lowest. Otherwise, meteorological parameters at the TM site were not different between the four trajectory clusters.

### 2.5. Potential source contribution function (PSCF)

Calculations of PSCF are similar to those described in other works.<sup>19,20</sup> The movement of an air parcel during sampling periods is described as segment endpoints of coordinates in terms of latitude and longitude. All the hourly endpoints in back trajectories generated by the HYSPLIT 4.8 were classified into 1 $^{\circ}$  latitude by 1 $^{\circ}$  longitude grid cells to avoid uncertainties in calculations. The PSCF value for the *ij*th cell was defined as:<sup>21</sup>

$$\text{PSCF}_{(i,j)} = m_{(i,j)}/n_{(i,j)},$$

where  $m_{(i,j)}$  is the number of endpoints corresponding to measured pollutant concentrations higher than a given criterion value, and  $n_{(i,j)}$  is the total number of endpoints falling in the grid cell. Given that air temperatures do not exert significant influence on the atmospheric concentrations of OCPs at TM, the mean value of each compound was chosen as a criterion value. All the PSCF values were plotted using mapping software (ArcGIS 9.2). Only cells including more than 10 total hourly points are displayed here.

## 3. Results and discussion

### 3.1. Concentrations and temporal variation

Monitored OCP levels in the air and concentration ratios are shown in Fig. 2–5. Mean air concentrations are compared with those reported for other background sites (Table 1). The average concentrations of OCPs and PCBs at TM were considerably higher than those measured at other background sites, except for  $\alpha$ -HCH ( $\alpha$ -hexachlorocyclohexane), which was comparable to those in other remote stations. The temperature-dependence<sup>22,23</sup>

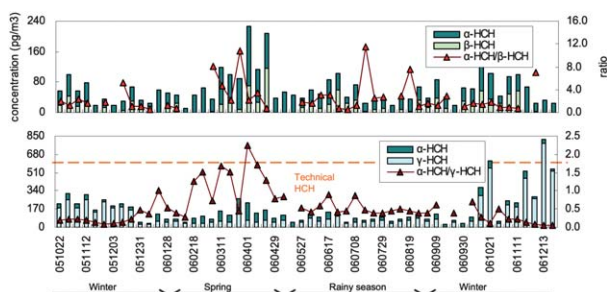


Fig. 2 Atmospheric concentrations of HCH isomers,  $\alpha$ -HCH/ $\beta$ -HCH and  $\alpha$ -HCH/ $\gamma$ -HCH ratios.

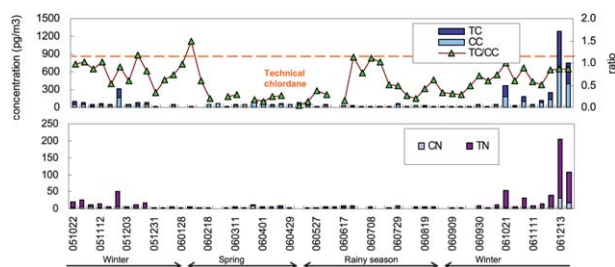


Fig. 3 Atmospheric concentrations of chlordanes and TC/CC ratio.

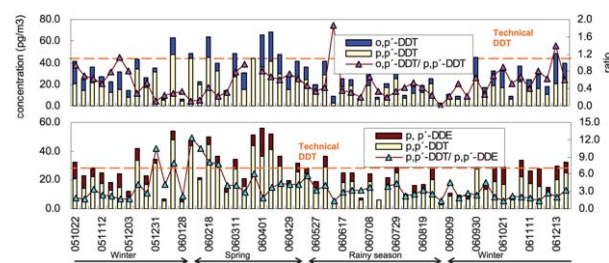


Fig. 4 Atmospheric concentrations of *o,p'*-DDT, *p,p'*-DDT and *p,p'*-DDE.

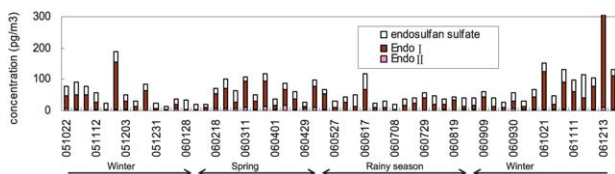


Fig. 5 Atmospheric concentration of endosulfan and endosulfan sulfate.

and influence of local meteorological conditions (air temperature, wind speed, and relative humidity)<sup>24</sup> on air concentrations of OCPs and PCBs was investigated using Pearson correlation analysis. No significant ( $p > 0.05$ ) or weak ( $r^2 < 0.4$ ) correlations were found between concentrations of the target compounds and meteorological factors, indicating that the local meteorology was of minor importance to the OCP and PCB atmospheric concentrations at TM.

Table 1 Comparison of mean OCPs concentrations (pg m<sup>-3</sup>) at TM with those in other background sites

	$\alpha$ -HCH	$\gamma$ -HCH	HCB	<i>o,p'</i> -DDT	<i>p,p'</i> -DDT	<i>p,p'</i> -DDE	TC	CC	TN	Endo I
TM (this study)	42	130	270	11	20	6.1	40	59	14	42
Mt Waliguan, China <sup>32</sup>	58.4	139	38.4	17.9	4.42	5.12	18.1	22.1	8.3	
Signy Island <sup>6</sup>	2.7	22		0.2	0.28	0.4	0.9	0.21	0.1	
Mt Everest <sup>31</sup>	44.2	7.1	16.7	7.1	3.5	0.68	0.03	0.09	0.08	75.4
Yahiko, Japan <sup>26</sup>	84	34	84		<2	1.3	14	15		
Alert, Canada <sup>30</sup>	13	1.7	52	0.22	0.14	0.3	0.25	0.64	0.35	5.6
Pallas, Finland <sup>30</sup>	9.9	2.8			0.25	0.58				
Storhofdi, Iceland <sup>30</sup>	2.7	3.8		0.11	0.14	0.16	0.082	0.11	0.079	
Zeppelin, Norway <sup>30</sup>	11	1.9	72	0.21	0.11	1.2	0.22	0.61	0.6	
Kinnigait, Canada <sup>30</sup>	27	3.1	47							3.3
Little Fox Lake <sup>30</sup>	48	4.5	67							8.3
Barrow, U.S.A. <sup>30</sup>	19	2.7	47							2.8
Valkarkai, Russia <sup>30</sup>				4.7	7.7					3.2
Nuuk, Greenland <sup>30</sup>	20	5.1				0.41	0.4	0.46		4.8
Tengchong <sup>44</sup>			62.6	4.7	2	2.9	7.8	8.3		

**3.1.1. HCH.** The atmospheric levels of  $\alpha$ -HCH have declined since technical HCH was prohibited worldwide.<sup>25–27</sup> The mean air concentration of  $\alpha$ -HCH at TM was  $42 \pm 26$  pg m<sup>-3</sup>, similar to values at other remote sites, for instance, in the Arctic,<sup>13,28,29</sup> the Tibetan plateau<sup>30</sup> and at Waliguan.<sup>10</sup> Elevated  $\alpha$ -HCH concentrations were observed from March to June 2006, while no significant temporal variation of  $\beta$ -HCH was observed (Fig. 2). Compared with the seasonal trend of other OCPs, the low variability in  $\alpha$ -HCH and  $\beta$ -HCH concentrations possibly suggests the elevated levels in spring were a result of enhanced surface–air exchange. Tropical Asia is considered to be the highest biomass-burning region during this period. A large proportion of burned area can be attributed to numerous fires related to slash-and-burn agricultural practices and land clearing. Therefore the burning-related volatilization of historical residues of  $\alpha$ -HCH and DDTs in spring could be another potential factor influencing atmospheric concentrations of the two compounds, which was also suggested in another report.<sup>31</sup> On the other hand, the mean  $\gamma$ -HCH air concentration was  $130 \pm 150$  pg m<sup>-3</sup>, considerably higher than data reported elsewhere<sup>13,14</sup> but similar to levels measured at Waliguan Baseline Observatory.<sup>10</sup> The concentration reached a maximum during winter, especially in 2006 (Fig. 2).

The isomer ratio of HCHs is an index frequently used to distinguish pollution sources. The ratio in air could be different from that in technical products due to evaporation from the surface, so vapour pressure-adjusted ratios are adopted here as criteria. The  $\alpha$ -HCH/ $\gamma$ -HCH ratio of technical HCH calibrated by relative vapour pressures at 25 °C is  $>1.9$ , while lindane contains more than 90% of  $\gamma$ -HCH,<sup>32</sup> and thus lowers the ratio. The average ratio of  $\alpha$ -HCH/ $\gamma$ -HCH was  $0.56 \pm 0.48$  at TM. A low  $\alpha$ -HCH/ $\gamma$ -HCH ratio with high  $\gamma$ -HCH concentrations occurred throughout winter (Fig. 2), implying a fresh input of lindane. However, ratios higher than those in the technical mixture and elevated  $\alpha$ -HCH concentrations were observed from February to April, indicating that there was likely an occurrence of technical HCH emission in the region, even though it was banned in the 1990s. Another HCH isomer,  $\beta$ -HCH, characterized by stronger chemical stability, is prone to resist degradation in the environment. Therefore, whether  $\alpha$ -HCH/ $\beta$ -HCH ratios are lower than the ratios of technical HCH is a commonly used

method to distinguish fresh or aged technical HCH sources. The average  $\alpha$ -HCH/ $\beta$ -HCH ratio at the TM site was 2.7, lower than the vapour pressure adjusted ratio in the technical mixture. This implies an influence of aged sources of technical HCH. Interestingly, a low  $\alpha$ -HCH/ $\beta$ -HCH ratio (<2) with a relatively high abundance of  $\beta$ -HCH was also observed occasionally, indicating that there might be some other unknown sources of  $\beta$ -HCH.

**3.1.2. Chlordane.** Atmospheric concentrations of individual chlordane ranged between 1.5–600  $\text{pg m}^{-3}$ , 2.3–690  $\text{pg m}^{-3}$ , 1.0–170  $\text{pg m}^{-3}$ , and 0.7–31  $\text{pg m}^{-3}$ , with median values of 11  $\text{pg m}^{-3}$ , 33  $\text{pg m}^{-3}$ , 4.9  $\text{pg m}^{-3}$  and 2.2  $\text{pg m}^{-3}$  for *trans*-chlordane (TC), *cis*-chlordane (CC), *trans*-nonachlor (TN) and *cis*-nonachlor (CN), respectively. These values were higher than previously reported background values (Table 1). The ratio of TC/CC has been used to identify the “age” of the substance.<sup>33</sup> The TC/CC ratio at TM was  $0.60 \pm 0.34$ , slightly higher than the ratios found in the Arctic<sup>34,35</sup> and lower than vapour pressure adjusted TC/CC ratio in technical chlordane at 25 °C.<sup>36</sup> The highest chlordane concentrations, as well as relatively high TC/CC ratios measured in winter, suggest fresh use of this OCP (Fig. 3), such as structure preservation in southern China. Nevertheless, significantly low TC/CC ratios and low TC concentration was observed in spring. Besides less application, the half life of chlordane is shorter compared with other OCPs. This could lead to a lower long-rang transport potential<sup>37</sup> and result in relatively low TC/CC ratios at TM in spring. During the rainy season, high TC/CC ratios indicate fresh sources but the atmospheric concentration levels were low.

**3.1.3. DDT.** DDT (dichlorodiphenyltrichloroethane) is a widely used OCP in south and southeast Asia. In this field

study, the mean air concentrations of *o,p'*-DDT, *p,p'*-DDT and *p,p'*-DDE averaged over the whole period of the campaign were  $10 \pm 7.1 \text{ pg m}^{-3}$ ,  $20 \pm 11 \text{ pg m}^{-3}$ , and  $6.1 \pm 3.5 \text{ pg m}^{-3}$ , respectively. As shown in Table 1, the concentrations of *o,p'*-DDT and *p,p'*-DDE (*p,p'*-Dichlorodiphenyldichloroethylene) were higher than the values in the Arctic and the Antarctic,<sup>13,14</sup> but lower than or analogous to those measured at other background sites around the Tibetan Plateau,<sup>10,15</sup> with the highest *p,p'*-DDT level in the present study. Although the measured air concentrations fluctuated little seasonally, the three related DDT compounds showed elevated concentrations in spring (Fig. 4). The relatively low concentrations were the result of a prohibition on the use of DDT in agriculture, but an exemption for malaria control in India and the MSA could lead to high DDT levels during the spring time.

The ratio of *p,p'*-DDT/*p,p'*-DDE is an index to evaluate the environmental transformation process of DDT. The *p,p'*-DDT/*p,p'*-DDE ratio at TM was above reported ratio of technical DDT at 25 °C<sup>38</sup> from January to February, 2006, suggesting fresh sources of DDT in this region. Besides technical DDT applied in south and southeast Asia,<sup>4</sup> another potential source of DDT is dicofol, which is an acaricide manufactured from technical DDT but contains more *o,p'*-DDT.<sup>39</sup> Through calculating the *o,p'*-DDT/*p,p'*-DDT ratio, we further estimate what fraction of DDT pollution is produced by dicofol and technical DDT. The *o,p'*-DDT/*p,p'*-DDT ratio in technical DDT is about 0.17–0.32.<sup>40</sup> This ratio can be increased through air–surface exchange<sup>38</sup> or by the influences of physicochemical processes before and during transport, so a ratio of 0.74–0.96 marks technical DDT use.<sup>38</sup> A ratio as low as  $0.53 \pm 0.32$  at TM suggests that technical DDT was the major source of DDT pollution during the sampling period.

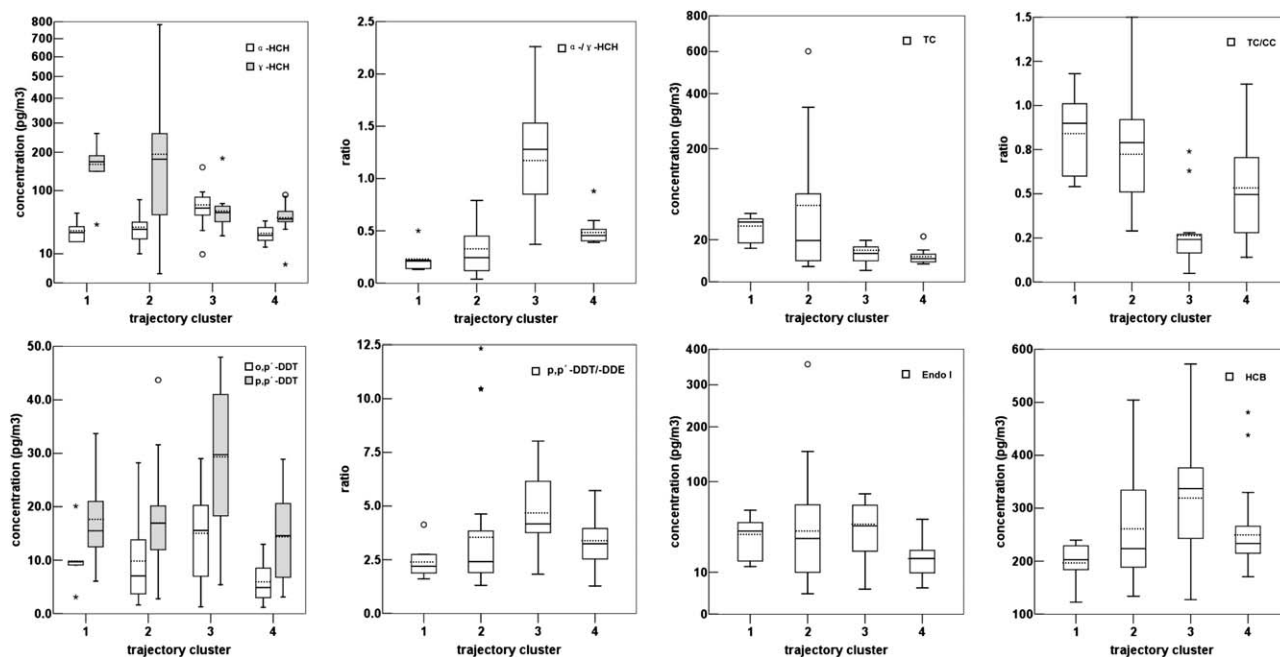


**Fig. 6** Box-whisker plots of atmospheric concentrations of pesticides from different source regions. The range of the box stands for the bounds of the 25th and 75th percentiles of the data. The dashed line within the box represents the mean value. The whiskers extending from the box symbolize the 10th and 90th percentiles of the data. Outliers that extend beyond the 10th and 90th percentiles are plotted individually. The concentrations of  $\alpha$ -HCH,  $\gamma$ -HCH, TC and Endo I are plotted in power scale with an exponent of 0.5.

**3.1.4. Endosulfan.** The usage of endosulfan has been increasing since this pesticide was first applied.<sup>4</sup> In general, air concentrations of endosulfan II (Endo II) and endosulfan sulfate are often below the method detection limit, thus are not reported for many remote sites, but the concentration level and temporal profile of endosulfan I (Endo I) in the Arctic demonstrates its ubiquitous character around the world.<sup>12</sup> The average concentrations of Endo I, Endo II and endosulfan sulfate at TM was  $42 \pm 54 \text{ pg m}^{-3}$ ,  $4.2 \pm 3.6 \text{ pg m}^{-3}$ , and  $24 \pm 11 \text{ pg m}^{-3}$ , respectively. Seasonal variation of Endo I was similar to that of chlordane (Fig. 5). The LRAT of POPs subject to

physicochemical properties, such as degradation rate and partitioning coefficients.<sup>41</sup> Significant correlations ( $r^2 = 0.588\text{--}0.996$ ,  $p = 0.001$ ) between chlordane,  $\gamma$ -HCH and Endo I were observed in this study in spite of their diverse physicochemical properties, indicating that their concentration variability is controlled by similar source region and transport pathways. Technical endosulfan contains about 70% of Endo I and 30% of Endo II,<sup>42</sup> both of which can degrade into endosulfan sulphate. However, endosulfan sulphate did not show a significant relationship with Endo I or Endo II, perhaps because endosulfan sulphate concentration reflects historical usage.

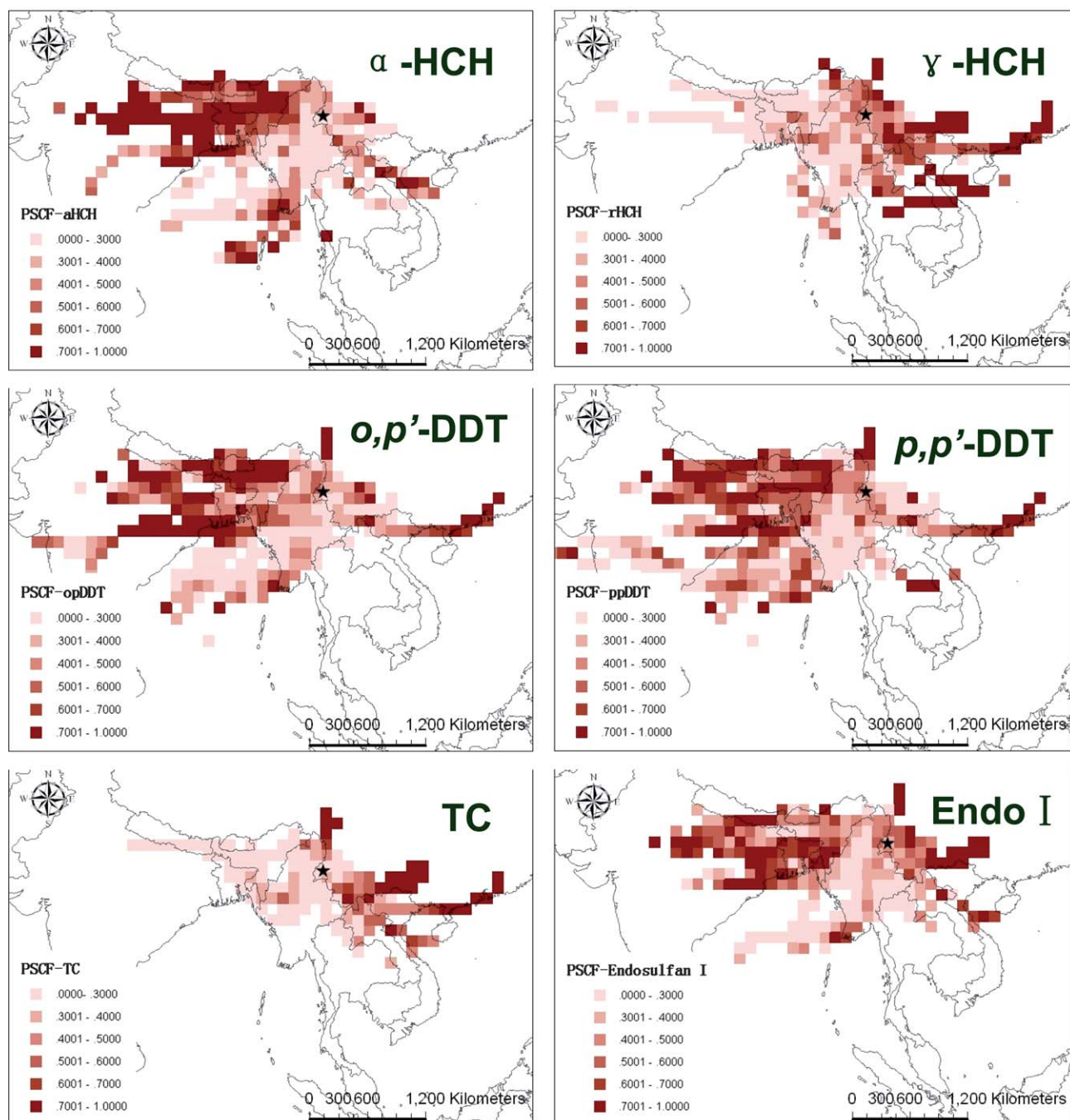


Fig. 7 Maps of potential sources of  $\alpha$ -HCH,  $\gamma$ -HCH, *o,p'*-DDT, *p,p'*-DDT, TC and Endo I. The darkness of red cells represents PSCF values.

**3.1.5. HCB.** Given the diversity of emission sources and its high thermodynamic stability,<sup>43</sup> HCB (Hexachlorobenzene) emerges everywhere in a variety of environmental media. Yet the concentration of HCB at TM site ( $270 \pm 100 \text{ pg m}^{-3}$ ) was higher than the concentrations reported in other remote areas (Table 1).

Despite the fact that concentrations of other OCPs reduced during the rainy season, HCB levels remained constant all year around. Because of the lack of temporal fluctuation, the high concentration of HCB reflects relatively high background levels in India, southern China and MSA.

**3.1.6. PCBs.** A total of 11 PCB congeners (IUPAC number 28, 49, 44, 37, 70, 66, 101, 99, 77, 114, 126) were detected in the samples. The annual mean air concentrations were  $22 \pm 10$ ,  $23 \pm 17$ ,  $8.6 \pm 9.0 \text{ pg m}^{-3}$  for tri-, tetra-, penta-chlorobiphenyls, respectively. Congener patterns of PCBs were characterized by a high proportion of tri-CBs, and tetra-CBs in China<sup>44</sup> and tetra-CBs and penta-CBs in India,<sup>6</sup> respectively. The dominance of tetra-CBs at TM differed from that in the other regions. Given that there was no significant seasonal variations in the magnitude of air concentrations of tri-, tetra- and penta-CBs, a prevalence of tetra-CBs at TM is consistent with the conclusion that PCB congeners with an intermediate degree of chlorination have greater LRAT potential than lower and heavier chlorinated PCBs.<sup>45</sup> Unlike OCPs, PCBs are assumed to be strongly affected by industrial activities which are irregularly distributed and constantly released pollutants. Consequently no significant temporal variation of PCB congeners was observed at TM.

### 3.2. Long-range atmospheric transport

LRAT could be the major factor that affected OCP and PCB concentrations at TM station. In order to assess the impact of distant sources on the sampling site, backward trajectories were clustered into four types by HYSPLIT 4.8 and measured composition data were grouped and plotted according to types of cluster in the backward trajectory analysis (Fig. 6). With analysis of variance (ANOVA), significant differences ( $p < 0.05$ ) were present in Fig. 6. It should be noted that the concentrations of  $\alpha$ -HCH,  $\gamma$ -HCH, TC and Endo I were plotted in power scale with an exponent of 0.5.

Type 1 trajectory, prevailing from October to December 2005, originated from the coast of southeastern China and the South China Sea, travelled across the northern part of Vietnam, Laos and Myanmar prior to arriving at TM. Under the northeast Asian monsoon regime, the air parcels brought relatively cold and dry air to TM. The average concentrations of OCPs were lower than or similar to those of type 2 and type 3 (Fig. 6). A low average ratio of  $\alpha$ -HCH/ $\gamma$ -HCH and a high average ratio of TC/CC confirm that lindane and technical chlordane were used currently when type 1 trajectory was prevailing. Interestingly, a low  $o,p'$ -DDT/ $p,p'$ -DDT ratio in this study, characteristic of technical DDT usage, is different from what was previously observed at the same observatory.<sup>44</sup> It is probable that DDT was brought to TM when air masses passed over regions with a high  $p,p'$ -DDT level.

The air mass cluster of type 2 mostly travelled across Myanmar and the northern region of Vietnam, Laos and Thailand. This cluster prevailed mostly in winter. The highest  $\gamma$ -HCH

concentrations were associated with type 2 air masses, especially when air came from MSA (Fig. 6). In addition, TC concentration associated with cluster 2 was higher than those associated with clusters 3 and 4 (Fig. 6). Positive correlations ( $r^2 = 0.67\text{--}0.99$ ,  $p < 0.001$ ) were observed between  $\gamma$ -HCH, chlordane and Endo I, all of which showed elevated concentrations during planting season, namely, spring and winter. The strong correlation and temporal pattern suggest the three compounds were related largely to agricultural activities in MSA when type 2 trajectories dominated air mass movement. In contrast, DDT-related compounds had a different temporal pattern.  $p,p'$ -DDT levels increased in spring and  $p,p'$ -DDE concentrations increased thereafter. In view of the  $p,p'$ -DDT/ $p,p'$ -DDE ratio, it is possible that technical DDT was used in spring and degraded to DDE later, owing to the intense sunlight and high temperatures in the tropics.

Trajectories of type 3, which prevailed from February to April, originated from central India, and passed through eastern India, Bangladesh, and northern Myanmar before arriving at TM. Significantly elevated levels of  $\alpha$ -HCH, DDTs, and endosulfan were associated with type 3 air masses (Fig. 6). The high concentration of HCH influenced by a type 3 cluster is a combined effect of LRAT of three kinds of HCH sources. The average ratio of  $\alpha$ -HCH/ $\gamma$ -HCH and  $\alpha$ -HCH/ $\beta$ -HCH (Fig. 6) suggests fresh technical HCH as a major source of HCH pollution. On the other hand, occasionally low  $\alpha$ -HCH/ $\gamma$ -HCH ratios accompanied with high levels of  $\gamma$ -HCH refers to lindane application. Low  $\alpha$ -HCH/ $\beta$ -HCH ratios with high  $\beta$ -HCH concentrations in some samples alludes to unknown sources of  $\beta$ -HCH, which were also observed in India (Paromita Chakraborty, unpublished data). Use of technical DDT was well supported by the present observation of low  $o,p'$ -DDT/ $p,p'$ -DDT, high  $p,p'$ -DDT/ $p,p'$ -DDE ratios and high  $p,p'$ -DDT concentrations (Fig. 6), while the air parcels travelled from the west through the eastern region of India before reaching TM. This is in good agreement with observations in Kolkata and Mumbai, two cities in India where these chemicals were still used. Elevated concentrations of Endo I and Endo II point to the application of endosulfan in central India.

The type 4 cluster is related to the Southern Asia (Indian) monsoon occurring mostly from May to August. During that time, air masses originated from the Arabian Sea, and passed over southern India, the Bay of Bengal and Myanmar. Most of the OCPs exhibited relatively low concentrations when air took this path to TM. The isomeric ratios of OCPs were more close to type 2 rather than type 3 (Fig. 6).

### 3.3. Identifying source regions of OCPs using PSCF model

Potential sources of OCPs are plotted in Fig. 7. In the PSCF maps, dark red cells represent high PSCF values. Since cells must meet the criteria of more than 10 hourly points, some potential source regions could be excluded in maps.

It can be inferred from the maps that India, northern MSA and southern China were the three major source regions. These three regions are characterized by prosperous agriculture and fledgling industries which would be consistent with the source regions of OCPs and PCBs. The region extending from central India to Bangladesh has been identified to be a source region of





- 37 A. Beyer, D. Mackay, M. Matthies, F. Wania and E. Webster, *Environ. Sci. Technol.*, 2000, **34**, 699–703.
- 38 X. Liu, G. Zhang, J. Li, L. L. Yu, Y. Xu, X. D. Li, Y. Kobara and K. C. Jones, *Environ. Sci. Technol.*, 2009, **43**, 1316–1321.
- 39 X. H. Qiu, T. Zhu, L. Jing, H. S. Pan, Q. L. Li, G. F. Miao and J. C. Gong, *Environ. Sci. Technol.*, 2004, **38**, 1368–1374.
- 40 R. L. Metcalf, *Organic insecticides: their chemistry and mode of action*, Interscience, N.Y, 1955.
- 41 F. Wania, *Environ. Sci. Technol.*, 2003, **37**, 1344–1351.
- 42 T. W. Burgoyne and R. A. Hites, *Environ. Sci. Technol.*, 1993, **27**, 910–914.
- 43 F. M. Jaward, N. J. Farrar, T. Harner, A. J. Sweetman and K. C. Jones, *Environ. Sci. Technol.*, 2004, **23**, 1355–1364.
- 44 T. M. Jaward, G. Zhang, J. J. Nam, A. J. Sweetman, J. P. Obbard, Y. Kobara and K. C. Jones, *Environ. Sci. Technol.*, 2005, **39**, 8638–8645.
- 45 L. Shen, F. Wania, Y. D. Lei, C. Teixeira, D. C. G. Muir and H. Xiao, *Environ. Pollut.*, 2006, **144**, 434–444.
- 46 G. Zhang, P. Chakraborty, J. Li, P. Sampathkumar, T. Balasubramanian, K. Kathiresan, S. Takahashi, A. Subramanian, S. Tanabe and K. C. Jones, *Environ. Sci. Technol.*, 2008, **42**, 8218–8223.
- 47 M. A. Matin, M. A. Malek, M. R. Amin, S. Rahman, J. Khatoon, M. Rahman, M. Aminuddin and A. J. Mian, *Agric. Ecosyst. Environ.*, 1998, **69**, 11–15.
- 48 T. Poolpak, P. Pokethitiyook, M. Kruatrachue, U. Arjarasirikoon and N. Thanwarliwat, *J. Hazard. Mater.*, 2008, **156**, 230–239.
- 49 J. Fu, B. Mai, G. Sheng, G. Zhang, X. Wang, P. a. Peng, X. Xiao, R. Ran, F. Cheng, X. Peng, Z. Wang and U. Wa Tang, *Chemosphere*, 2003, **52**, 1411–1422.
- 50 H. Iwata, S. Tanabe, N. Sakal and R. Tatsukawa, *Environ. Sci. Technol.*, 1993, **27**, 1080–1098.
- 51 I. Stemmler and G. Lammel, *Geophys. Res. Lett.*, 2009, **36**, L24602.